SCIEPublish

Article

Photocatalytic and Photothermal Catalytic Oxidation of Ethene and Ethanol Using TiO_2-Based Catalysts under UV-C and UV-A Irradiation

Ravinraj Adaikan Ovannan, Frederic Dappozze and Chantal Guillard *

IRCELYON, UMR 5256, CNRS, Universite Claude Bernard Lyon 1, F-69100 Villeurbanne, France; ravin1153@gmail.com (R.A.O.); frederic.dappozze@ircelyon.univ-lyon1.fr (F.D.)

* Corresponding author. E-mail: chantal.guillard@ircelyon.univ-lyon1.fr (C.G.)

Received: 27 June 2024; Accepted: 9 August 2024; Available online: 28 August 2024

ABSTRACT: Photocatalytic (PCO) and photothermocatalytic oxidation (PTCO) of ethene (C_2H_4) and ethanol (EtOH) are investigated using TiO_2 and 1%Pt/TiO_2 coating on velvet glass support in the presence of UV-A and UV-C irradiation. Both VOC are efficiently mineralised under UV-A irradiation and PCO, but the presence of Pt has a minor impact on their transformation. Instead, there is only a slight increase in the disappearance of EtOH and the formation of acetaldehyde, which are already observed in the dark. Surprisingly, when a higher photon flux is emitted with a UV-C lamp, photocatalytic disappearance and mineralisation of EtOH are less effective than under UV-A irradiation in the presence or absence of Pt. Similar behaviour is also observed on C_2H_4 PCO in the presence of 1%Pt/TiO_2 but not on its PCO mineralisation with TiO_2, which is improved by a factor equivalent to the number of photons emitted. Under PTCO, by increasing the temperature from 40 °C to 120 °C, only a benefit impact is observed on C_2H_4 and EtOH disappearance but an important decrease of mineralization of C_2H_4 was observed in presence of TiO_2 and UV-C The behaviour of these two VOCs under different irradiations and temperatures will be discussed according to the catalytic process.

Keywords: Photocatalysis; Photothermocatalysis; Ethene; Ethanol; TiO_2; Pt/TiO_2; Temperature; UV-A; UV-C

1. Introduction

Volatile organic compounds (VOCs) are colourless organic chemicals released in the gas state due to their high volatility and low boiling point, such as acetone, carbon disulphide, ethene (C_2H_4), ethanol (EtOH), formaldehyde, toluene and, xylene. C_2H_4 is a natural ripe-causing hormone of plants that helps grow and develop fruits and vegetables. It is a persistent pollutant in the Food and Vegetable (F&V) industry as it causes rapid maturation and deterioration in the storing environment at low temperatures, leading to food waste and money [1]. Meanwhile, EtOH is an emerging pollutant mainly due to the COVID-19 pandemic, increasing its rapid production and emission into the atmosphere due to its high volatility in the last two years. EtOH-based disinfectants can release around 6000 ppb to 8000 ppb in a closed area in an hour [2]. Prolonged exposure to the vast EtOH amount could lead to health risks and other environmental problems. Therefore, reducing the C_2H_4 to prolong F&V's shelf life and airborne EtOH content in the atmosphere is necessary.

Moving towards sustainable and greener goals, photocatalytic oxidation (PCO) and photothermal catalytic oxidation (PTCO) of VOCs, especially C_2H_4 and EtOH in the gas phase, have gained attention among researchers to control the VOCs' content in the atmosphere. When the photocatalyst absorbs light, PCO is a redox reaction carried out by photogenerated species, such as holes (h^+) and electrons (e). In the case of PCO, h^+ plays a central role since it oxidises VOCs into CO_2 [3], and e^- reduces O_2 into $O_2^{\circ-}$ which can also oxide VOC and avoids charge recombination. Similarly, PTCO is an extension of PCO, but it is carried out in the presence of light and heat energy generated either internally by photothermal materials or externally by a heat source [4]. In other words, it is similar to a combination of photocatalysis and thermal catalysis, i.e., catalysis at high temperatures without light irradiation. Thus, the oxidation of C_2H_4 and EtOH via photocatalysis and photothermal catalyst can be expressed as Equations (1) and (2).

https://doi.org/10.35534/prp.2024.10006

$$C_2H_4 + 3O_2 \rightarrow 2CO_2 + 2H_2O \quad (1)$$

$$C_2H_5OH + 3O_2 \rightarrow 2CO_2 + 3H_2O \quad (2)$$

The most common catalyst used for PCO [5–8] and PTCO [9–13] is titanium dioxide alone or coupled with other materials, mainly metals such as Pt, Ag, Au, Ni to enhance the reaction efficiency Other common catalysts are also used in PTCO alone or coupled with TiO_2 such as ZnO, WO_3, and C_3N_4, CeO_2, bismuth-based photocatalysts,etc. [14–21]. Most of these are semiconductors because they possess a unique electronic structure with adequate band gap (Eg) that produces the photogenerated species, h^+ and e^-, through migration between valence band (VB) and conduction band (CB) during the photon irradiation, unlike metals and insulators. Primary recent phothermocatalytic researches deal with CO_2 conversion, CH_4 activation, NH_3 synthesis, and water splitting [4] or solar light in the presence of plasmon, allowing plasmonic localised heating [22].

Some studies have been carried out in oxidising C_2H_4 and EtOH using photocatalysis. Park et al. carried out gas-phased C_2H_4 PCO using TiO_2 in ultrafine powder. They studied the factors affecting the reaction and found anatase TiO_2 with a larger surface area, a big Eg and many hydroxyl groups result in higher reaction efficiency [23]. Similar observations were obtained using TiO_2 for photocatalytic oxidation of VOCs, especially C_2H_4 [24,25].

Furthermore, in Park et al.'s study [23], platinised TiO_2 with about 1wt% showed better C_2H_4 PCO than the unplatinised one with higher selectivity towards CO_2 without intermediates. Similarly, Vorontsov and Dubovitskaya observed a double increment in the reaction rate of EtOH PCO by Pt-loaded TiO_2 [26], supported by Murcia et al.[27]. However, Fraters et al. [28] showed that the effect of Pt nanoparticles largely depends on the substrate's molecular functionality. For example, they found that Pt reduces the propane PCO activity, whereas a positive effect is observed on EtOH PCO. Publications on the effect of UV irradiation with different wavelengths and photon emission rates on gaseous C_2H_4 and EtOH oxidation or another VOC are rare. Pathak et al. [29] mentioned that UV-C lamp with higher photon emission and shorter wavelength produces complete oxidation of C_2H_4, unlike under UV-A. However, the UV-C lamp used is not only 254 nm but also a wavelength of 185 nm and Farhanian et al. [30] show a different behaviour between UV-C lamps, including 185 nm or not on EtOH PCO. In particular, crotonaldehyde is formed in the presence of 185 nm but not observed under only 254 nm. The works of Couts et al. on EtOH [31] and Kaneva et al. [32] on C_2H_4 PCO show that UV-C light gives a higher conversion degree owing to the higher photon energy than UV-A light.

Apart from photocatalysis, platinum (Pt) loading on TiO_2 has greatly interested experts in photothermal catalysis. Pt is a non-plasmonic material [33] and has been shown to enlarge the catalyst's absorption spectrum from UV to visible light, which drives both photon flux (UV and Visible flux) and heat energy during the PTCO [34]. Zorn et al. studied a mixture of TiO_2 and ZrO_2 as a catalyst over temperatures below 110 °C on PTCO of C_2H_4 [35]. They found that platinum catalyst improves the photocatalytic reaction of ethene from a temperature above 70 °C. Fu et al. support the idea that platinised catalysts have a vast potential for photothermal catalytic applications through their study on C_2H_4 [36]. However, neither of these publications mentions whether there is a synergy between photocatalysis and thermocatalysis for C_2H_4 degradation and mineralisation or the impact of light sources on PTCO.

On the other hand, Kennedy and Datye [37], investigating EtOH PTCO using Pt/TiO_2, found that the complete oxidation into CO_2 significantly surpasses the combined contribution of photo-oxidation over TiO_2 and thermal processes. They suggest that Pt thermal activity for acetaldehyde oxidation, formed from EtOH on TiO_2, becomes significant on Pt/TiO_2, favouring the oxidation pathway to CO_2 [37]. These results agree with the works of Vorontsov et al. [26], which showed that acetaldehyde oxidation is favoured on Pt/TiO_2. Besides, the effect of the Pt loading method on the PTCO reaction is discussed in their work. The photo-reduced approach, i.e., photodeposition of Pt on the catalyst, results in higher EtOH conversion and CO_2 mineralisation than the thermal reduction method, i.e., impregnation or adsorption.

Our study aims to understand better the impact of Pt, temperature and nature of light (UV-C and UV-A) on the conversion and mineralisation of two VOC, C_2H_4 and EtOH using TiO_2 coated on a velvet glass support and determine (i) if activation of photocatalyst under UV-C allow improving the PCO and PTCO of these both VOC, (ii) if the presence of Pt is essential, (iii) if a synergy is really obtained between photocatalysis and thermal catalysis and finally (iv) if a general behaviour of the impact of these parameters can be generalised.

2. Experimental Setup

2.1. Materials

Commercia TiO_2, Hombikat UV-100, is purchased from Sachtleben Chemie. It is a pure anatase phase with a surface area of about 300 m^2/g. Around 18 cm × 10 cm glass velvet is used as support, supplied by the industrial partner, TREFFLER. Hydrogen hexachloroplatinate (IV) hydrate is purchased from SigmaAldrich (Saint Louis, Missouri, USA)® to synthesise platinised catalyst. C_2H_4 (497 ppmV in the air) and EtOH (1040 ppmV in air) are purchased in gas cylinders from Air Liquide and Messer.

2.2. Deposition of Catalyst on the Glass Velvet Support

Glass velvet from Treffler company has been used as support (Figure 1). The glass velvet is washed with distilled water and oven-dried at 200 °C overnight. An aqueous suspension of TiO_2 is sprayed on the dry velvet and dried at 200 °C overnight on the velvet's surface. About 4 mg/cm^2 measured by ICP-OES was coated on velvet support.

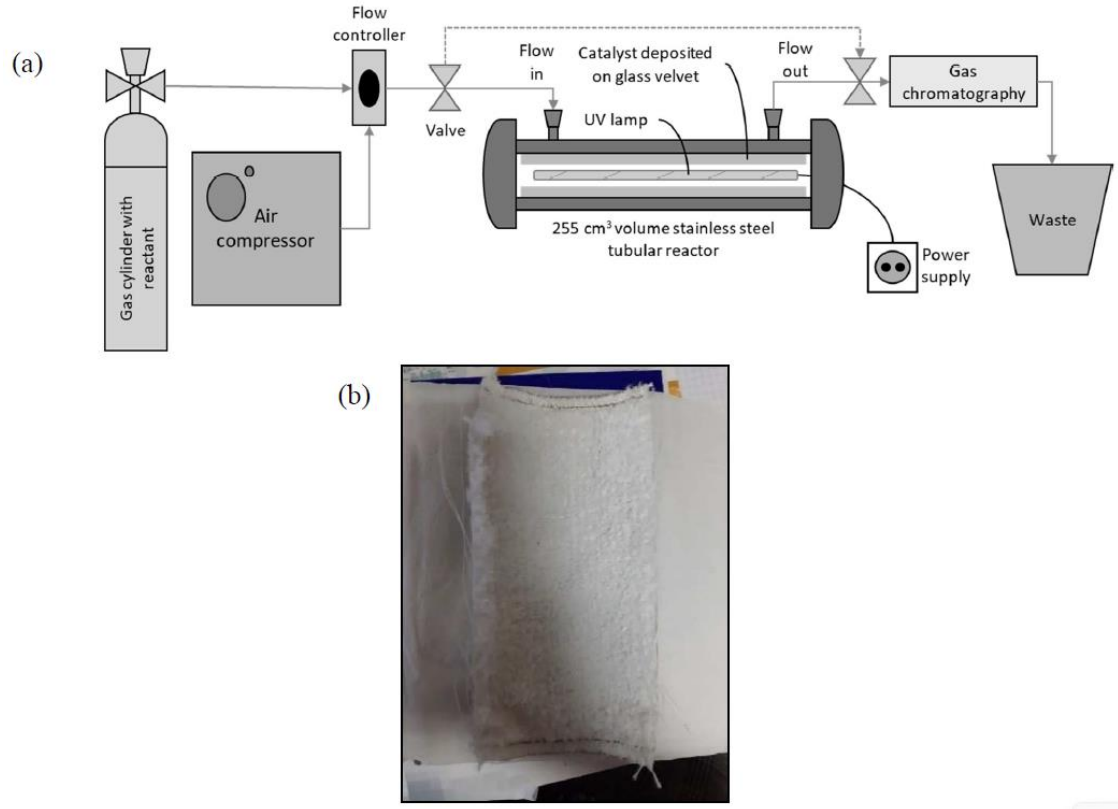

Figure 1. Schematic diagram of the experimental setup for the photocatalytic test using a 255 cm^3 volume stainless steel tubular reactor with UV lamp (**a**) and catalyst supported on glass velvet support (**b**).

2.3. Synthesis of Platinised TiO_2

A sample of Pt/TiO_2 is prepared under photo-deposition using about 1% of Pt, which is the best for photothermal catalysis [26]. The photodeposition method is based on M. Yamamoto et al. [38]. Around 5.76 g of TiO_2 (Hombikat UV-100) is mixed in 100 mL of distilled water. Similarly, 0.46 g of hydrogen hexachloroplatinate (IV) hydrate is measured as a Pt precursor and added to the TiO_2 suspension. EtOH with a concentration of 13.06 M is measured at 2.3 mL and added to the suspension as a hole scavenger. The mixture is illuminated under a UV-C lamp under continuous stirring and 10 mL/min argon purging for 72 h. Then, the suspension is centrifuged and dried at 200 °C in the oven overnight. The resulting catalyst is labeled as photo-reduced 1wt% Pt/TiO_2.

2.4. Photocatalytic and Photothermal Catalytic Test

Both tests are carried out in a stainless steel tubular reactor with a length of 27 cm. The light source (UV lamp) is mounted inside the reactor using a removable quartz glass tube with an outer diameter of 2 cm. There is a space between the glass tube and the reactor wall to place the glass velvet, the industrial support from which the catalyst is deposited.

The total volume of the reactor available for VOC is 255 cm^3. Each side end of the reactor is screwable, allowing the users to change the catalyst accordingly, as shown in Figure 1. For photothermal catalytic tests, the tubular reactor is wrapped with a heating pad connected to a thermocouple and temperature controller for the heat supply, while the photocatalytic tests are carried out without it. Two UV lamps, Vilber-Lourmat (L = 265 mm, diameter = 15 mm) are utilised in the study: UV-A (365 nm) and UV-C (254 nm). The resulting stream from the reactor is analysed using GC FID Varian 3800 and GC FID-PDHID Clarus 500 for C_2H_4 and EtOH oxidation, respectively.

VOC, C_2H_4 or EtOH, is directly supplied from a gas tank and mixed with compressed air, composed of oxygen and nitrogen at 8 bar. A flowrate of 1 litre/min of VOC at different concentrations is used for the tests. Photocatalytic tests are done without heating. However, the UV lamp produces heat, causing a temperature rise from 25 °C to around 50 °C. Besides, the temperature range studied for the photothermal catalytic test is from 50 °C to 130 °C in both dark and UV irradiance. Since the photocatalysis is observed at 50 °C under UV irradiance, photothermal catalysis is studied at temperatures above the PC's temperature with an external heating supply. For the photothermal catalytic test, the temperature is increased to the desired value once the VOC enters the reactor. The UV lamp is turned on after reaching the adsorption-desorption equilibrium without UV irradiation.

Before every test, the glass-supported catalyst is treated and cleansed under the irradiance of a UV-C lamp and air flowrate of 200 mL/min overnight inside the reactor. Then, the test is started with the VOC concentration until stabilisation at the desired concentration for about 1 to 1.5 h without passing through the reactor (Step 1). It is followed by flowing the VOC stream into the reactor using valves to reach adsorption-desorption equilibrium on the glass-supported catalyst's surface for about 4 h (Step 2) before turning on the UV lamp (Step 3). For photothermal catalytic tests, stabilisation at the desired temperature is carried out simultaneously using the controller attached to the heating pad. Thermal catalysis or VOC catalytic oxidation, if any, is studied in the dark until equilibrium was reached. Then, the UV lamp is turned on, and VOC oxidation is carried out for 4 h.

VOC conversion (%), product yields (%C) and mineralisation (%) are calculated as follows:

$$Conversion\ (\%) = \frac{VOC\ degraded}{Initial\ VOC} \times 100\%$$

$$Product\ i\ (\%C) = \frac{Product\ i\ concentration}{VOC\ degraded\ concentration} \times \frac{Product\ i\ carbon\ number}{2} \times 100\%$$

$$Mineralisation(\%) = \frac{CO_2\ formed\ (ppbV)}{VOC\ degraded\ and\ absorbed\ (ppbV) \times 2} \times 100\%$$

2.5. Analytical Procedure

2.5.1. Analysis of VOC

Ethene and CO_2 concentrations are monitored on a Varian ((Agilent Technologies, Palo Alto (CA) USA)) 3800 GC-FID system with an automated injection gas valve using a 500 µL loop. Columns used are a Varian CPSil-5 (50 m × 30 mm × 1.2 µm) followed by SupleQPlot (Supelco − 30 m × 0.32 mm × 15 µm). The injector and oven are set at 30 °C for all the analysis. Helium is used as a gas vector (4.4 mL/min). The FID detector (Varian inc., Agilent Technologies, Palo Alto (CA) USA)) (250 °C) is preceded by a methanization module made of heated (400 °C) nickel powder heated under hydrogen flow.

EtOH is analysed with a Clarus 500 gas chromatograph (Perkin Elmer, Waltham, MA, USA). Separation occurs on an RT-Q-Bond column (25 m × 0.53 mm × 20 µm). The oven is set at 50 °C then heated at 20 °C/min to 200 °C. A Polyarc® (Activated Research Company, Eden Prairie, MN, USA) module is used as an oxidiser/methanizer to transform all carbonated molecules into CO_2 and methane before FID (250 °C) detection.

2.5.2. Analysis of the Number of Photons

A CCD Spectrometer Avantes AvaSpec-ULS2048 (Avantes B.V., Apeldoorn, The Netherlands) is used to measure the emission spectra of both lamps. Before the analysis, a calibration is carried out using a Deuterium Halogen Light Source. Light intensities received by the catalyst have been determined using a VLX-3W radiometer equipped with a UVA–365 nm ± 10 nm probe and UVC_254 ± 10 nm, depending of the lamp used. Optical properties of both UV lamps are given in Table 1.

Table 1. Optical properties of UV lamps.

Parameters	UV-A	UV-C
Lamp surface area	122.5 cm^2	
Irradiance on support surface	3.54 $mWatt/cm^2$	8.7 $mWatt/cm^2$
Luminous power	0.434 W	1.066 W
Photon flux	$8 \times 10^{17} \pm 1$ photons/s	$13.6 \times 10^{17} \pm 1.4$ photons/s

3. Result and Discussion

3.1. Photocatalytic Degradation (PCO)

3.1.1. Comparison of C_2H_4 and EtOH Photocatalytic Oxidation (PCO)

PCO of C_2H_4 and EtOH have been studied in the presence of platinised and unplatinised TiO_2 Hombikat coated on velvet glass. The profiles of C_2H_4 and C_2H_5OH concentration versus time during PCO in the presence of unplatinised TiO_2 Hombikat are shown in Figure 2a,b.

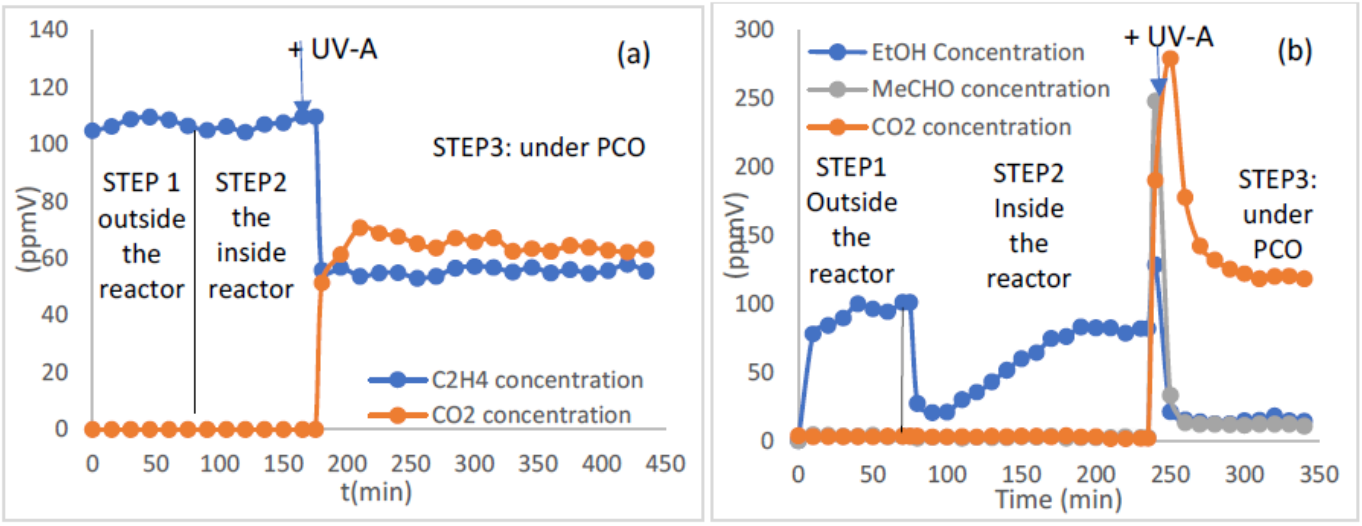

Figure 2. Profile of C_2H_4 concentration (**a**) and C_2H_5OH concentration (**b**) versus time during PCO in the presence of 100 ppmV of VOC and TiO_2 Hombikat coated on velvet glass.

Depending on the VOC type, after overnight UV treatment, a distinct photocatalytic pattern is observed for each degradation on the velvet glass (Figure 2). After the first step (Step 1) of VOC stabilisation outside the reactor, no or negligible adsorption of C_2H_4 on photocatalytic material was detected after introducing C_2H_4 into the reactor where the catalyst is placed (Step 2), but adsorption of EtOH occurs. This behavior is due to the presence of the OH group in EtOH favoring hydrogen bonds with the surface of the hydrated catalyst. Moreover, after achieving adsorption equilibrium, EtOH does not return to its initial concentration, suggesting dissociative EtOH adsorption on TiO_2 [39,40]. About 17% of EtOH appears to be irreversibly adsorbed. At the same time, no CO_2 concentration or new compound is detected during these two steps for both VOCs.

Once the UV lamp is illuminated (Step 3), the concentration of CO_2 shoots up while both VOC concentration decreases, reaching equilibrium as time goes by. As for EtOH, the formation of acetaldehyde (MeCHO) is detected as a by-product, whereas no by-product was observed with C_2H_4, including the formation of formaldehyde not detected in our analytical conditions or other products remaining adsorbed. Indeed, in the given conditions, only 60% was mineralised (Table 2). Table 2 indicates the adsorption, conversion, mineralisation and by-product detected during the PCO of C_2H_4 and EtOH.

Table 2. Percentage of conversion, mineralisation and by-product detected during PCO of C_2H_4 and EtOH in the presence of TiO_2 Hombikat. Remarks: All % conversion, mineralisation and by-products are taken into account of the initial concentration of VOC disappeared and not the VOC concentration after adsorption.

VOC (TiO_2 Hombikat)	VOC Adsorbed % Adsorbed	VOC Converted % Conversion	CO_2 % Mineralisation	MeCHO % by-Product
C_2H_4	<1	48%	60%	/
EtOH	13%	88%	67%	11%

It is also crucial to highlight that some nonidentified by-products are formed but less extended compared to C_2H_4 degradation. The comparison of PCO of EtOH and ethene shows that EtOH is more easily degraded than C_2H_4 but that both VOC are not entirely mineralised in the given conditions.

3.1.2. Impact of the Presence of Pt/TiO_2 on C_2H_4 and EtOH PCO

Results of PCO of C_2H_4 and EtOH in the presence of 1%Pt/TiO_2 Hombikat are reported in Table 3 and compared to those obtained without platinium in Table 2.

Table 3. % of conversion, mineralisation and by-product detected during PCO of C_2H_4 and C_2H_5OH in the presence of 1%Pt/TiO_2 Hombikat. Remarks: all % conversion, mineralisation and by-products are taken into account of the initial concentration of VOC disappeared and not the VOC concentration after adsorption.

VOC (1%Pt/TiO_2 Hombikat)	% Transformed Under Dark	% Conversion	% Mineralisation	% CH_3CHO
C_2H_4	<1	48%	65%	/
EtOH	50%	95%	67%	13%

Pt loading on TiO_2 seems to have no or slight improvement in the conversion and mineralisation of C_2H_4 and et OH (Figure3a,b). Specifically, the presence of Pt seems to improve the mineralisation of C_2H_4 and the conversion of EtOH slightly. However, a significant impact on the EtOH adsorption is observed in the presence of 1%Pt/TiO_2 (Figure 3c), approximately 50% compared to 13% in the absence of Pt with a slight increase of MeCHO formation, which may correspond to the slight improvement in C_2H_5OH conversion.

The impacts from the Pt on C_2H_4 oxidation at near ambient temperature is in agreement with the works of Zorn et al. [35,36] and with the observation of Fraters et al., showing that the effect of Pt nanoparticles on TiO_2 is mainly dependent on the nature of the substrate by working with propane and EtOH [28]. However, Pt has a negative impact on propane oxidation, an essential improvement of EtOH oxidation, and a more critical formation of acetaldehyde and mineralisation. They attributed this difference to the strong adsorption of EtOH on the TiO_2 surface, likely forming ethoxy groups and inhibiting oxygen activation over TiO_2. In this case, the presence of Pt enormously improved the EtOH adsorption but only slightly the formation of MeCHO. However, under irradiation at a temperature of about 40–45 °C induced by the lamp's heat, only a slight improvement of EtOH oxidation is noted, while no improvement in CO_2 was observed. Likely, ethoxy groups are formed, as Fraters et al. [28] suggested, but seem to have only a little or no impact on photocatalysis at this temperature.

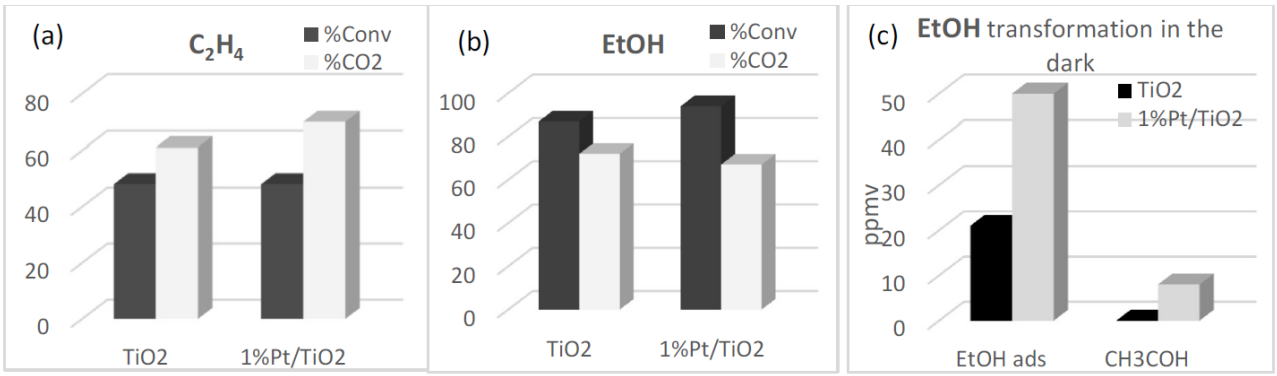

Figure 3. Comparison of the C_2H_4 (**a**) and EtOH (**b**) PCO in the presence of TiO_2 Hombikat and 1%Pt/TiO_2 under UV-A. Adsorption of EtOH and formation of CH_3COH in the dark in the presence of TiO_2 Hombikat and 1%Pt/TiO_2 (**c**).

3.1.3. Impact of UV Light Type

The effect of UV-A and UV-C lamps is studied for the PCO of C_2H_4 and EtOH in the presence of TiO_2 and 1%Pt/TiO_2 (Figure 4).

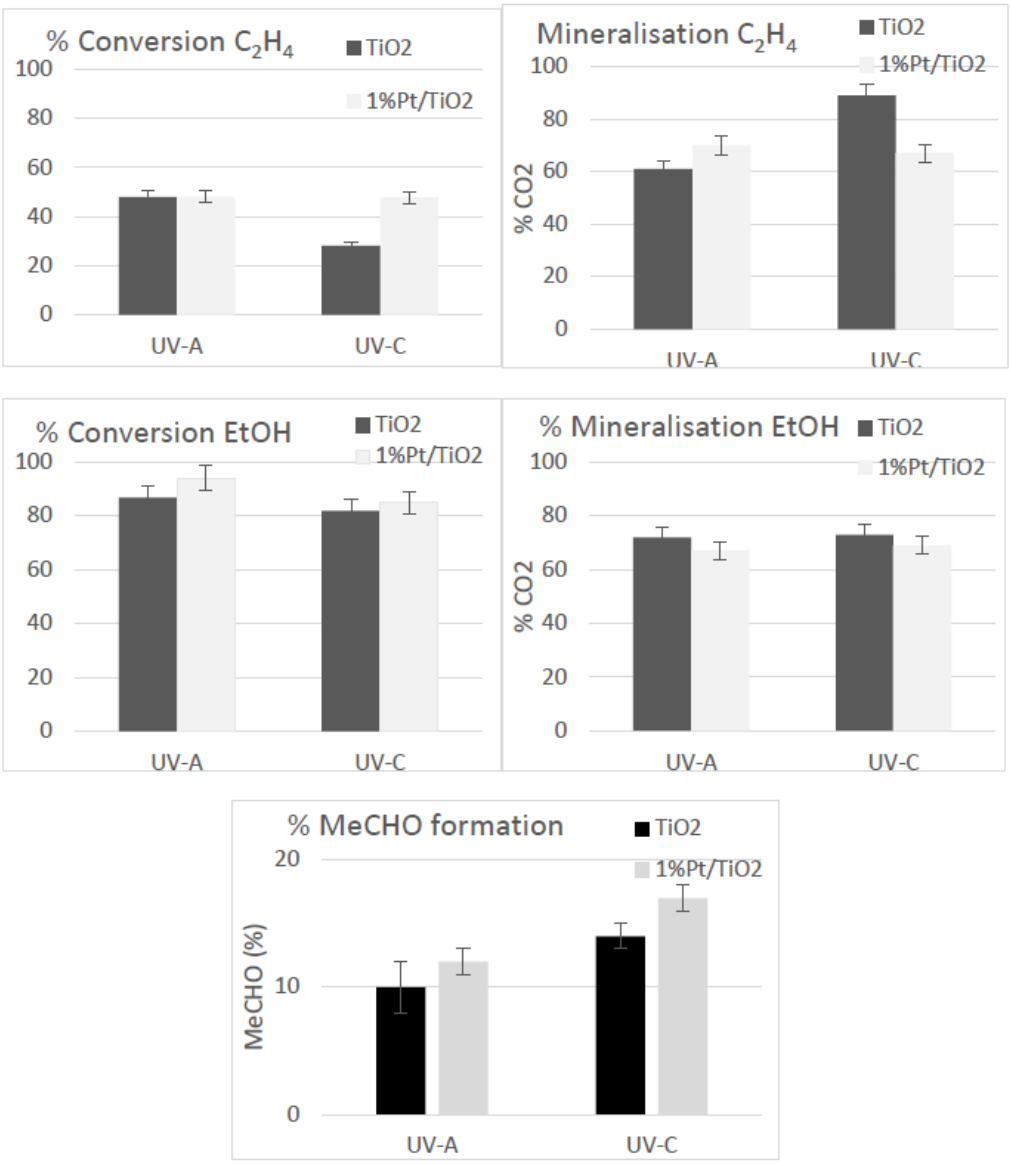

Figure 4. Comparison of C_2H_4 and EtOH conversion and mineralisation and formation of CH_3COH in the presence of TiO_2 Hombikat and 1%Pt/TiO_2 under UV-A and UV-C. Remarks: The conversion and mineralisation of EtOH are calculated based on the initial concentration that disappeared.

In the presence of unplatinised and platinised TiO_2, no improvement in the conversion of both VOC is obtained under UV-C, where a higher photon flux is emitted. A detrimental effect has even been observed in the degradation of C_2H_4. These behaviours are unlike the expected results. A higher photon generation should enable a higher (e^--h^+) pair generation, improving conversion [30,41–45], contradicting the study's findings. However, a higher percentage of mineralisation was observed in the presence of C_2H_4 and unplatinised TiO_2, suggesting the degradation of by-products under the UV-C lamp.

Moreover, with both catalysts, the UV-C lamp improves the formation of MeCHO. The difference observed between the behaviour of C_2H_4 and EtOH under UV-C is not due to the double bond in C_2H_4, which could favour photochemistry over photocatalysis. In fact, the PCO of C_2H_6 has the same behaviour as C_2H_4, where its conversion is less efficient in the presence of UV-C irradiation (Figure 5). Therefore, the absence of an increase in the efficiency under UV-C could be explained by the limitation of the catalyst activation by UV-C due to its lower penetration in the velvet glass compared to UV-A due to the nature of support which is in Quartz and can absorb UV-C and not UV-A.

In the case of Pt/TiO_2, the conversion and mineralisation are less impacted, probably due to the catalyst's darker grey colour limiting the penetration of both UV. These are just hypotheses; further study is required on the UV lamp effect.

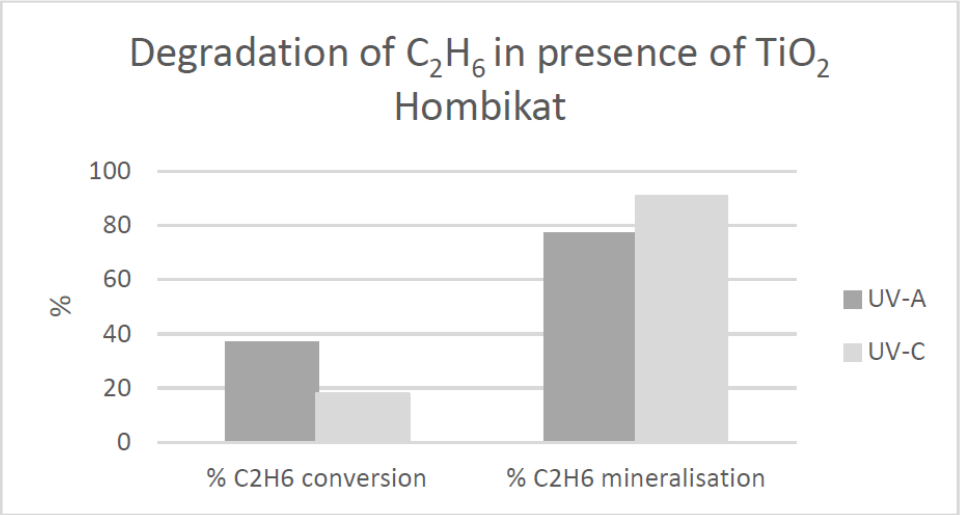

Figure 5. Photocatalytic degradation of ethane (C_2H_6) in the presence of TiO_2 UV-100 (Hombikat) under UV-A and UV-C.

3.2. Photothermal Catalytic Test (PTCO)

The impact of temperature on C_2H_4 and EtOH degradation is studied using TiO_2 UV-100 (Hombikat) unplatinized (Figure 6) and platinised (1% Pt/TiO_2) (Figure 7). It is important to note that when the lamp is on, the temperature in the reactor is approximately 50 °C. So, the initial PTCO temperature of 50 °C corresponds to PCO since it is due to the heat from the UV lamp solely without any external heating source.

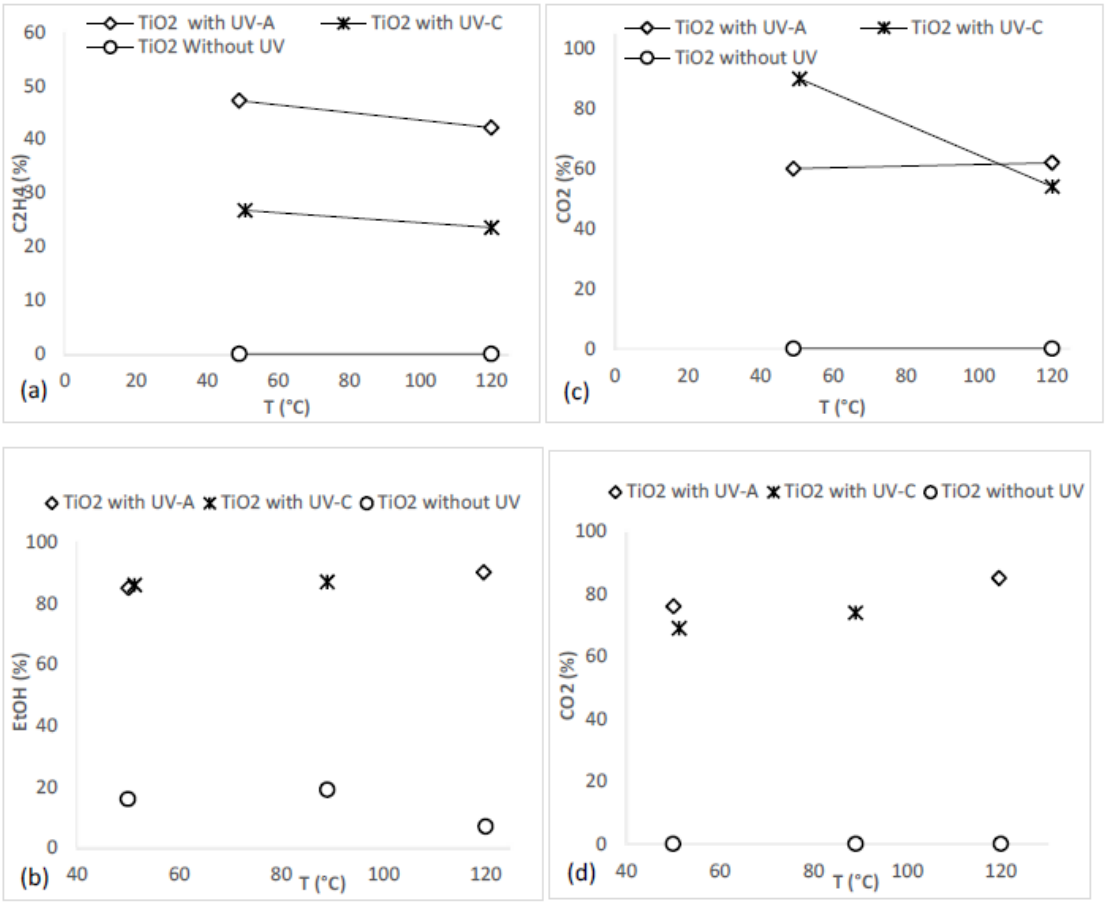

Figure 6. Impact of temperature in the presence of UV-A or UV-C or absence of light on conversion (**a**,**b**) and mineralisation (**c**,**d**) of C_2H_4 (**a**,**c**) and EtOH (**b**,**d**) in the presence of TiO_2 Hombikat.

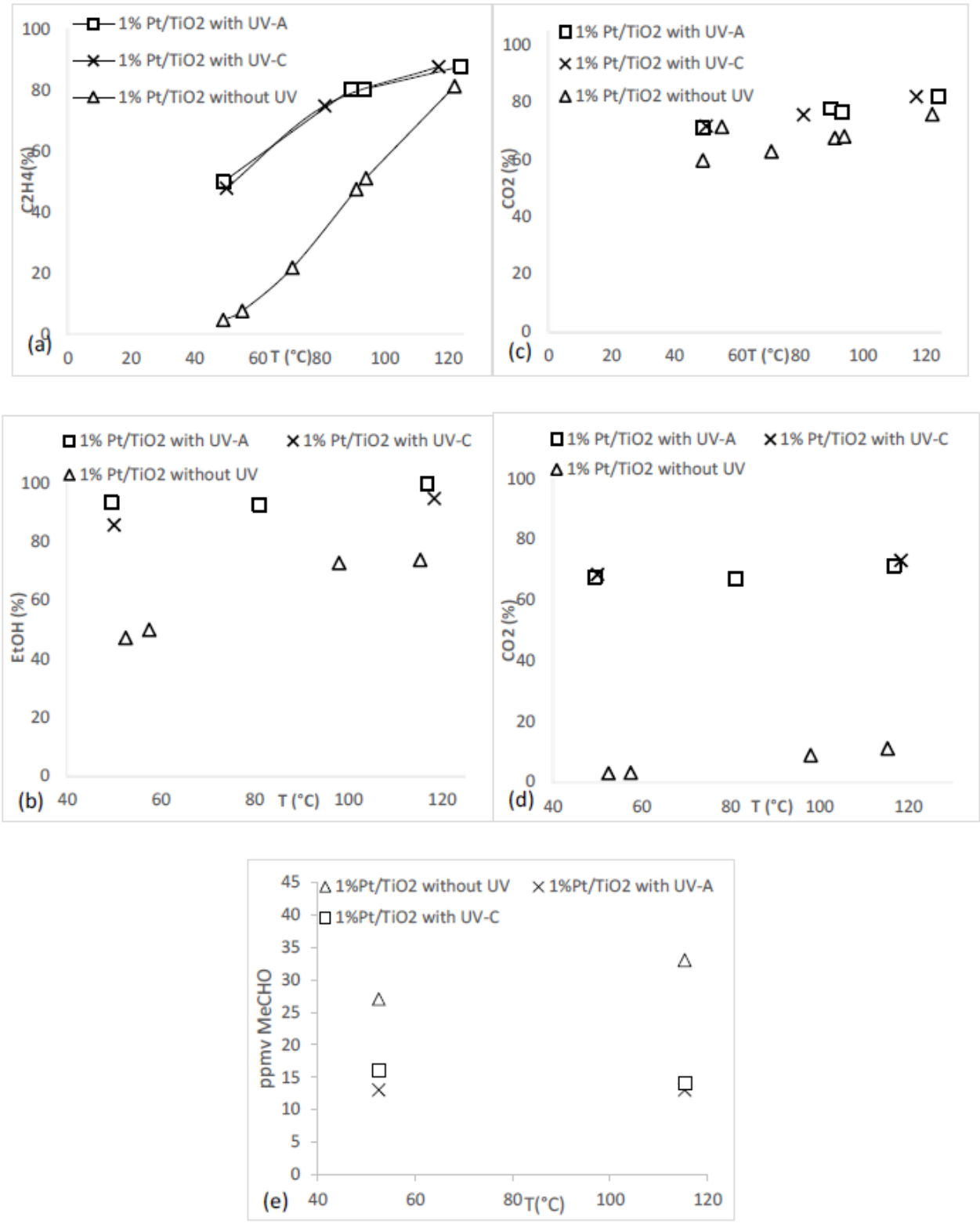

Figure 7. Impact of temperature in the presence of UV-A or UV-C or absence of light on conversion (**a**,**b**) and mineralisation (**c**,**d**) of C_2H_4 (**a**,**c**) and EtOH (**b**,**d**) and on the formation of MeCHO (**e**) in the presence of 1%Pt/TiO_2 Hombikat.

In the presence of unplatinised TiO_2, whether under UV (UV-A or UV-C) or in the dark, temperature does not affect the conversion of C_2H_4 and EtOH (Figure 6a,b). Moreover, while temperature does not affect mineralisation under UV-A and UV-C during the EtOH degradation (Figure 6d) and under UV-A during the C_2H_4 degradation, there is a significant reduction in mineralisation of C_2H_4 observed under UV-C (Figure 6b). This lower activity could be resulted from the formation of the precursor of polymer such as propylene or butene favoured with temperature [46–49] and under UV-C irradiation [50,51].

A different behaviour is observed when 1% Pt is present on TiO_2. In the presence or absence of UV, a significant increase in C_2H_4 and EtOH conversion is observed (Figure 7a,b), and to a lesser extent in the mineralisation (Figure

7c,d). In the dark, the conversion of C_2H_4 is already increased from a few % at 50 °C and continues to increase to more than 80% at 120 °C while the mineralisation increases from 60% to 75%. In the case of EtOH, the conversion is improved from 47% to 74% while the mineralisation increases from about 3% to 11%.

Based on the comparison study between platinised and unplatinised catalysts, platinised catalyst exhibits better efficiency than the unplatinised one under illumination at increasing temperature, reaching the highest C_2H_4 conversion and CO_2 mineralisation of 88% and 83%, respectively, at 124 °C. In the dark, the unplatinised catalyst does not display any activity but platinised one demonstrates catalytic oxidation through thermal catalysis as temperature increases. Until 90 °C, its conversion efficiency is lower than unplatinised one exposed to UV-A, then its performance increases, while its CO_2 mineralisation increases with the temperature. Therefore, it is evident that 1% Pt/TiO_2 causes the catalyst to exhibits both photo and thermal catalytic activity, producing a photothermal catalyst.

Like C_2H_4 PTCO, Pt with 1%Pt on TiO_2 increases the catalyst's performance in the EtOH PTCO at a similar temperature range. Platinised catalysts exhibit thermal-assisted photocatalysis, where the reaction is driven mainly by light, with heat assisting it [33]. It is because unplatinised catalysts have better activity under UV irradiance than platinised catalysts in the dark, indicating that heat boosts photocatalysis rather than driving it simultaneously, as in C_2H_4 PTCO. Another significant observation is that platinised catalysts produce more MeCHO without UV irradiation than the unplatinised ones. It is mainly due to the thermal catalytic oxidation observed during the formation of MeCHO by the Pt catalyst in the dark. However, under UV irradiation, its formation is limited (Figure 7e).

Therefore, the study's results agree with several studies indicating Pt loading increases the photocatalyst's performance in PTCO conversion of C_2H_4 [35,36] and EtOH [26,37], provided that the temperature is higher than about 70–80 °C. These works show that photocatalysis and thermal catalysis drive the reaction simultaneously. However, the word "synergy" used in some publications [12,33,52] dealing with photothermocatalysis does not correspond to our results. Indeed, in this case, the activity is not greater than the contribution from photo-oxidation over TiO_2 plus thermal oxidation over Pt. Is they a synergy in the studies of photothermocatalysis due to the different types of mechanism (plasmonic localised heating, thermal vibration of molecules and non-radiative relaxation in semiconductors) or to the type of reaction used (inert atmosphere against air in our reaction)? It would be fascinating to explore this behaviour further.

4. Conclusions

The photocatalytic degradation (PCO) and photo-thermocatalytic degradation (PTCO) of C_2H_4 and EtOH are studied using glass velvet impregnated using TiO_2 UV-100, with or without 1% Pt under UV-A or UV-C irradiation. Significant differences in the adsorption of volatile organic compounds (VOCs) in the absence of light, as well as variations depending on the presence of Pt on TiO_2, are observed. While C_2H_4 is little adsorb onto either catalyst, EtOH shows notable adsorption, especially on 1%Pt/TiO_2 (50%) and to a lesser extent on non-platinized TiO_2 (13%). Adsorption is dissociative in both cases, forming acetaldehyde in the presence of 1%Pt/TiO_2.

Under PCO UV-A irradiation, EtOH is converted approximately two times faster than C_2H_4 in the presence of TiO_2, although their mineralisation is relatively similar. Approximately 60 to 70 ppmv of these VOCs are mineralised under our specific flux and light power conditions. The presence of 1% Pt on TiO_2 seems to have only little effect on VOCs' photocatalytic conversion and mineralisation.

Under PCO UV-C, although its photon flux is higher, neither the conversion nor the mineralisation of VOCs is improved on Pt or non-Pt TiO_2. Unexpectedly, the conversion of C_2H_4 is even halved under UV-C while its mineralisation is improved, indicating a preference for the degradation of by-products formed under UV-C. This behaviour is also observed during the degradation of ethane, suggesting that the presence of a double bond on C_2H_4 is not the cause of this efficiency decrease. This behaviour in the presence of PCO UV-C compared to PCO UV-A could be explained by the lower penetration of UV-C compared to UV-A. In the case of 1%Pt/TiO_2, the conversion and mineralisation are less impacted, probably due to the darker grey colour of the catalyst limiting the penetration of both UV types. These are just hypotheses; further study is required on the effect of UV lamps.

Under PTCO in the presence of TiO_2, temperature appears to have no beneficial effect on converting C_2H_4 and EtOH. It even has a detrimental impact on C_2H_4 mineralisation under UV-C, attributed to the formation of precursors of polymers such as propylene or butene favored by temperature and UV-C. A different behavior is observed when 1%Pt is present on TiO_2. So, the presence of Pt in TiO_2 appears essential for PTCO reaction. Through thermal catalysis, Pt enables the elimination and mineralisation of C_2H_4 from around 50 °C, while it mainly promotes the adsorption of EtOH and, to a lesser extent, the formation of acetaldehyde. Due to the catalytic properties of Pt, the disappearance of these two VOCs, and to a lesser extent, their mineralisation, is improved under "photothermocatalysis". However, can

we speak of the synergy between photocatalysis and catalysis? Isn't it simply the addition of these two types of reactions that we call "photothermocatalysis"? It is also important to emphasise that at 120 °C, these two reactions are equally effective, and beyond this temperature, photonic activation loses its interest. However, it is important to highlight the impact of temperature in the presence of Pt/TiO_2 under UV-C, which helps to avoid the decrease in efficiency probably due to its impact on the formation of polymer precursor. This impact will need to be further explored in the future.

Author Contributions

Conceptualization, C.G.; Methodology, C.G. and F.D.; Validation, C.G.; Formal Analysis, R.A.O. and F.D.; Investigation, R.A.O.; Data Curation, C.G.; Writing–Original Draft Preparation, R.A.O.; Writing–Review & Editing, C.G.; Visualization, C.G.; Supervision, C.G.; Funding Acquisition, C.G.

Ethics Statement

Not Applicable.

Informed Consent Statement

Not Applicable.

Funding

This research received no external funding.

Declaration of Competing Interest

The authors declare that they have no known competing financial interests or personal relationships that could have appeared to influence the work reported in this paper.

References

1. Qi Y, Li C, Li H, Yang H, Guan J. Elimination or Removal of Ethene for Fruit and Vegetable Storage via Low-Temperature Catalytic Oxidation. *J. Agric. Food Chem.* **2021**, *69*, 10419–10439. doi:10.1021/acs.jafc.1c02868.
2. Jiang J, Ding X, Isaacson KP, Tasoglou A, Huber H, Shah AD, et al. Ethanol-based disinfectant sprays drive rapid changes in the chemical composition of indoor air in residential buildings. *J. Hazard. Mater. Lett.* **2021**, *2*, 100042. doi:10.1016/j.hazl.2021.100042.
3. Zhang J, Tian B, Wang L, Xing M, Lei J. *Photocatalysis: Fundamentals, Materials and Applications*; Springer: Singapore, 2018; Volume 100. doi:10.1007/978-981-13-2113-9.
4. Song C, Wang Z, Yin Z, Xiao D, Ma D. Principles and applications of photothermal catalysis. *Chem. Catal.* **2022**, *2*, 52–83. doi:10.1016/j.checat.2021.10.005.
5. Masresha G, Jabasingh SA, Kebede S, Doo-Arhin D, Assefa M. A review of prospects and challenges of photocatalytic decomposition of volatile organic compounds (VOCs) under humid environment. *Can. J. Chem. Eng.* **2023**, *101*, 6905–6918. doi:10.1002/cjce.24978.
6. Shayegan Z, Lee C-S, Haghighat F. TiO_2 photocatalyst for removal of volatile organic compounds in gas phase—A review. *Chem. Eng. J.* **2018**, *334*, 2408–2439. doi:10.1016/j.cej.2017.09.153.
7. Ji-Won Y, Kumar V, Dae-Hwan L, Swati V, Deepak K, Hassan A, et al. Photocatalytic potential of a titanium dioxide–supported platinum catalyst against VOCs with complicated composition under varying humidity conditions. *J. Clean. Prod.* **2022**, *371*, 133487. doi:10.1016/j.jclepro.2022.133487.
8. Keller V, Bernhardt P, Garin F. Photocatalytic oxidation of butyl acetate in vapor phase on TiO_2, Pt/TiO_2 and WO_3/TiO_2 catalysts. *J. Catal.* **2003**, *215*, 129–138. doi:10.1016/S0021-9517(03)00002-2.
9. Zhou Y, Doronkin DE, Zhao Z, Plessow PN, Jelic J, Detlefs B, et al. Photothermal Catalysis over Nonplasmonic Pt/TiO_2 Studied by Operando HERFD-XANES, Resonant XES, DRIFTS. *ACS Catal.* **2018**, *8*, 11398–11406. doi:10.1021/acscatal.8b03724.
10. Zhang J, Chen H, Duan X, Sun H, Wang S. Photothermal catalysis: From fundamentals to practical applications. *Mater. Today* **2023**, *68*, 234–253. doi:10.1016/j.mattod.2023.06.017.
11. Mateo D, Cerrillo J-L, Durini S, Gascon J. Fundamentals and applications of photothermal catalysis. *Chem. Soc. Rev.* **2021**, *50*, 2173–2210. doi:10.1039/D0CS00357C.

12. Keller N, Ivanez J, Highfield J, Ruppert AM. Photo-/thermal synergies in heterogeneous catalysis: Towards low temperature (solar-driven) processing for sustainable energy and chemicals. *Appl. Catal. B Environ.* **2021**, *296*, 120320. doi:10.1016/j.apcatb.2021.120320.
13. Trzeciak M, Miądlicki P, Tryba B. Enhanced Degradation of Ethene in Thermo-Photocatalytic Process Using TiO_2/Nickel Foam. *Materials* **2024**, *17*, 267. doi:10.3390/ma17010267.
14. Tahir M, Tasleem S, Tahir B. Recent development in band engineering of binary semiconductor materials for solar driven photocatalytic hydrogen production. *Int. J. Hydrogen Energy* **2020**, *45*, 15985–16038. doi:10.1016/j.ijhydene.2020.04.071.
15. Daniele S, Ghazzal MN, Hubert-Pfalzgraf LG, Duchamp C, Guillard C, Ledoux G. Preparations of nanoparticles, nano-composites and fibers of ZnO from an amide precursor: Photocatalytic decomposition of (CH3)2S2 in a continuous flow reactor. *Mater. Res. Bull.* **2006**, *41*, 2210–2218. doi:10.1016/j.materresbull.2006.04.041.
16. Yu J, Caravaca A, Guillard C, Vernoux P, Zhou L, Wang L, et al. Carbon nitride quantum dots modified TiO_2 inverse opal photonic crystal for solving indoor VOCs pollution. *Catalysts* **2021**, *11*, 464. doi:10.3390/catal11040464.
17. Chang B, Tang L, Zhang X, Li J, Shen Z, Lyu J. Optimisation of photothermal conversion and catalytic sites for photo-assisted-catalytic degradation of volatile organic compounds. *Chemosphere* **2023**, *310*, 136696. doi:10.1016/j.chemosphere.2022.136696.
18. Ren L, Li Y, Liu H, Zhao C, Zhao X, Xie H. Intensitive UV–Vis-IR driven catalytic activity of Pt supported on hierarchical ZnO porous nanosheets for benzene degradation via novel photothermocatalytic synergetic effect. *J. Environ. Chem. Eng.* **2022**, *10*, 107694. doi:10.1016/j.jece.2022.107694.
19. Zhang N, He W, Cheng Z, Lu J, Zhou Y, Ding D, et al. Construction of α-MnO_2/g-C_3N_4 Z-scheme heterojunction for photothermal synergistic catalytic decomposition of formaldehyde. *Chem. Eng. J.* **2023**, *466*, 143160. doi:10.1016/j.cej.2023.143160.
20. Yu E, Li J, Chen J, Chen J, Hong Z, Jia H. Enhanced photothermal catalytic degradation of toluene by loading Pt nanoparticles on manganese oxide: Photoactivation of lattice oxygen. *J. Hazard. Mater.* **2020**, *388*, 121800. doi:10.1016/j.jhazmat.2019.121800.
21. Ma S, Luo X, Ran G, Li Y, Cao Z, Liu X, et al. Defect engineering of ultrathin 2D nanosheet BiOI/Bi for enhanced photothermal-catalytic synergistic bacteria-killing. *Chem. Eng. J.* **2022**, *435*, 134810. doi:10.1016/j.cej.2022.134810.
22. Luo S, Ren X, Lin H, Song H, Ye J. Plasmonic photothermal catalysis for solar-to-fuel conversion: Current status and prospects. *Chem. Sci.* **2021**, *12*, 5701–5719. doi:10.1039/D1SC00064K.
23. Park D-R, Ahn B-J, Park H-S, Yamashita H, Anpo M. Photocatalytic oxidation of ethene to CO_2 and H_2O on ultrafine powdered TiO_2 photocatalysts: Effect of the presence of O_2 and H_2O and the addition of Pt. *Korean J. Chem. Eng.* **2001**, *18*, 930–934. doi:10.1007/BF02705621.
24. Vorontsov AV, Kabachkov EN, Balikhin IL, Kurkin EN, Troitskii VN, Smirniotis PG. Correlation of Surface Area with Photocatalytic Activity of TiO_2. *J. Adv. Oxid. Technol.* **2018**, *21*, 127–137. doi:10.26802/jaots.2017.0063.
25. Tibbitts TW, Cushman KE, Fu X, Anderson MA, Bula RJ. Factors controlling activity of zirconia-titania for photocatalytic oxidation of ethene. *Adv. Space Res.* **1998**, *22*, 1443–1451. doi:10.1016/s0273-1177(98)00214-2.
26. Vorontsov AV, Dubovitskaya VP. Selectivity of photocatalytic oxidation of gaseous ethanol over pure and modified TiO_2. *J. Catal.* **2004**, *221*, 102–109. doi:10.1016/j.jcat.2003.09.011.
27. Murcia JJ, Hidalgo MC, Navío JA, Vaiano V, Ciambelli P, Sannino D. Photocatalytic Ethanol Oxidative Dehydrogenation over Pt/TiO_2: Effect of the Addition of Blue Phosphors. *Int. J. Photoenergy* **2012**, *2012*, e687262. doi:10.1155/2012/687262.
28. Fraters BD, Amrollahi R, Mul G. How Pt nanoparticles affect TiO_2-induced gas-phase photocatalytic oxidation reactions. *J. Catal.* **2015**, *324*, 119–126. doi:10.1016/j.jcat.2015.01.023.
29. Pathak N, Rux G, Geyer M, Herppich W, Rauh C, Mahajan P. Effect of light wavelength and TiO_2 on photocatalytic removal of ethene under low oxygen and high humidity storage conditions. *Acta Hortic.* **2018**, *1194*, 1345–1352. doi:10.17660/ActaHortic.2018.1194.189.
30. Farhanian D, Haghighat F, Lee C-S, Lakdawala N. Impact of design parameters on the performance of ultraviolet photocatalytic oxidation air cleaner. *Build. Environ.* **2013**, *66*, 148–157. doi:10.1016/j.buildenv.2013.04.010.
31. Coutts JL, Levine LH, Richards JT, Mazyck DW. The effect of photon source on heterogeneous photocatalytic oxidation of ethanol by a silica–titania composite. *J. Photochem. Photobiol. Chem.* **2011**, *225*, 58–64. doi:10.1016/j.jphotochem.2011.09.026.
32. Kaneva NV, Bojinova AS, Papazova KI, Dimitrov DT, Eliyas AE. Investigation of photocatalytic properties of pure and Ln (La^{3+}, Eu^{3+}, Ce^{3+})–modified ZnO powders synthesised by thermal method. *Bulg. Chem. Commun.* **2017**, *49*, 172–176.
33. Ma R, Sun J, Li DH, Wei JJ. Review of synergistic photo-thermo-catalysis: Mechanisms, materials and applications. *Int. J. Hydrogen Energy* **2020**, *45*, 30288–30324. doi:10.1016/j.ijhydene.2020.08.127.
34. Song R, Luo B, Liu M, Geng J, Jing D, Liu H. Synergetic coupling of photo and thermal energy for efficient hydrogen production by formic acid reforming. *AIChE J.* **2017**, *63*, 2916–2925. doi:10.1002/aic.15663.
35. Zorn ME, Tompkins DT, Zeltner WA, Anderson MA. Catalytic and Photocatalytic Oxidation of Ethene on Titania-Based Thin-Films. *Environ. Sci. Technol.* **2000**, *34*, 5206–5210. doi:10.1021/es991250m.

36. Fu X, Clark LA, Zeltner WA, Anderson MA. Effects of reaction temperature and water vapor content on the heterogeneous photocatalytic oxidation of ethene. *J. Photochem. Photobiol. Chem.* **1996**, *97*, 181–186. doi:10.1016/1010-6030(95)04269-5.
37. Kennedy JC, Datye AK. Photothermal Heterogeneous Oxidation of Ethanol over Pt/TiO_2. *J. Catal.* **1998**, *179*, 375–389. doi:10.1006/jcat.1998.2242.
38. Yamamoto M, Minoura Y, Akatsuka M, Ogawa S, Yagi S, Yamamoto A, et al. Comparison of platinum photodeposition processes on two types of titanium dioxide photocatalysts. *Phys. Chem. Chem. Phys.* **2020**, *22*, 8730–8738. doi:10.1039/C9CP06988G.
39. Ma Z, Guo Q, Mao X, Ren Z, Wang X, Xu C, et al. Photocatalytic Dissociation of Ethanol on TiO_2(110) by Near-Band-Gap Excitation. *J. Phys. Chem. C* **2013**, *117*, 10336–10344. doi:10.1021/jp309925x.
40. Shepot'ko ML, Davydov AA. Forms of adsorption of ethanol on anatase and paths of their transformation. *Theor. Exp. Chem.* **1991**, *27*, 210–214. doi:10.1007/bf01372479.
41. Lee J-M, Kim M-S, Kim B-W. Photodegradation of bisphenol-A with TiO_2 immobilised on the glass tubes including the UV light lamps. *Water Res.* **2004**, *38*, 3605–3613. doi:10.1016/j.watres.2004.05.015.
42. Doná G, Dagostin JLA, Takashina TA, de Castilhos F, Igarashi-Mafra L. A comparative approach of methylparaben photocatalytic degradation assisted by UV-C, UV-A and Vis radiations. *Environ. Technol.* **2018**, *39*, 1238–1249. doi:10.1080/09593330.2017.1326528.
43. Matthews RW, McEvoy SR. Photocatalytic degradation of phenol in the presence of near-UV illuminated titanium dioxide. *J. Photochem. Photobiol. Chem.* **1992**, *64*, 231–246. doi:10.1016/1010-6030(92)85110-G.
44. Puma GL, Yue PL. Enhanced Photocatalysis in a Pilot Laminar Falling Film Slurry Reactor. *Ind. Eng. Chem. Res.* **1999**, *38*, 3246–3254. doi:10.1021/ie9807607.
45. Herrmann J-M. Heterogeneous photocatalysis: Fundamentals and applications to the removal of various types of aqueous pollutants. *Catal. Today* **1999**, *53*, 115–129. doi:10.1016/S0920-5861(99)00107-8.
46. Ghashghaee M, Shirvani S. Catalytic transformation of ethene to propylene and butene over an acidic Ca-incorporated composite nanocatalyst. *Appl. Catal. A: Gen.* **2019**, *569*, 20–27. doi:10.1016/j.apcata.2018.10.017.
47. Lin B, Zhang Q, Wang Y. Catalytic Conversion of Ethene to Propylene and Butene over H-ZSM-5. *Ind. Eng. Chem. Res.* **2009**, *48*, 10788–10795. doi:10.1021/ie901227p.
48. Andrei RD, Popa MI, Fajula F, Cammarano C, Al Khudhair A, Bouchmella K, et al. Ethene to Propylene by One-Pot Catalytic Cascade Reactions. *ACS Catal.* **2015**, *5*, 2774–2777. doi:10.1021/acscatal.5b00383.
49. Beucher R, Cammarano C, Rodríguez-Castellón E, Hulea V. Direct conversion of ethene to propylene over Ni- and W-based catalysts: An unprecedented behaviour. *Catal. Commun.* **2020**, *144*, 106091. doi:10.1016/j.catcom.2020.106091.
50. Barzan C, Mino L, Morra E, Groppo E, Chiesa M, Spoto G. Photoinduced Ethene Polymerization on Titania Nanoparticles. *ChemCatChem* **2017**, *9*, 4324–4327. doi:10.1002/cctc.201700850.
51. Purohit PV, Rothschild M, Ehrlich DJ. UV Enhancement of Surface Catalytic Polymerization of Ethene. *MRS Proc.* **1988**, *129*, 259. doi:10.1557/proc-129-259.
52. Wei L, Yu C, Yang K, Fan Q, Ji H. Recent advances in VOCs and CO removal via photothermal synergistic catalysis. *Chin. J. Catal.* **2021**, *42*, 1078–1095. doi:10.1016/s1872-2067(20)63721-4a.